Eur. Phys. J. C 55, 273–283 (2008)
DOI 10.1140/epjc/s10052-008-0584-8

THE EUROPEAN
PHYSICAL JOURNAL C

Regular Article – Theoretical Physics

On the radiative pion decay

Rene Unterdorfer[1,a], Hannes Pichl[2]

[1] Paul Scherrer Institut, WHGA/128, 5232 Villigen PSI, Switzerland
[2] Helvetia Insurance, Dufourstrasse 40, 9001 St. Gallen, Switzerland

Received: 10 February 2008 /
Published online: 19 April 2008 –

Abstract. A reanalysis of the radiative pion decay together with the calculation of the radiative corrections within chiral perturbation theory (CHPT) is performed. The amplitude of this decay contains an inner Bremsstrahlung contribution and a structure-dependent part, which are both accessible in experiments. In order to obtain a reliable estimate of the hadronic contributions we combine the CHPT result with a large-N_c expansion and experimental data on other decays, which makes it possible to determine the occurring coupling constants.

PACS. 13.20.Cz; 12.39.Fe

1 Introduction

Rare decays are a useful source of information on particle interactions. Searches for new physics effects can take place at the high-energy or the high-precision frontier. At low energies new heavy particles can appear in the quantum loops. The advantage of high-precision physics is that one does not need to know the particle content of possible new physics in order to detect discrepancies between experimental results and theoretical predictions. One works with known external particles. On the other hand, it is of course not possible to detect new particles directly at low energies.

The radiative pion decay $\pi^+ \to e^+\nu_e\gamma$ is interesting as it is not dominated by inner Bremsstrahlung and therefore sensitive to the so-called "structure-dependent" contributions that are generated by QCD effects. These are described with the help of two form factors, the vector and the axial-vector form factor. Via the conserved-vector-current (CVC) hypothesis the vector form factor can be related to the decays $\pi^0 \to \gamma\gamma$ and $\pi^0 \to \gamma e^+e^-$, in which cases already precise data exist [1]. Therefore it is possible to measure the axial-vector form factor in experiments on the radiative pion decay directly. If one extracts both form factors experimentally with high precision, deviations from the CVC hypothesis can be investigated. Isospin breaking effects are of interest as they are not completely understood in the case of two-pion electroproduction and the corresponding τ decay. There has been a discussion on a possible tensor interaction that could be detected in experiments on radiative pion decay [2, 3]. The induced tensor form factor due to radiative corrections is expected to be very small, but an explicit calculation seems to be useful.

The typical energy scale of pion decays lies far below the region where perturbative standard model calculations are possible. At low energies, chiral perturbation theory (CHPT) [4–7] is used as the effective field theory of the standard model in this energy region. All high-energy effects are included in the coupling constants of the effective Lagrangian. If it is not possible to determine all these coupling constants by the use of experimental data from other processes, large-N_c QCD [8] is used to estimate them.

Previous theoretical calculations at two-loop order of the structure-dependent contributions to the radiative pion decay have been presented in [9, 10]. The lowest-order radiative corrections that are relevant for the inner Bremsstrahlung part are given in [11]. We complete the analysis by calculating the radiative corrections to the structure-dependent part within the framework of CHPT to lowest order in the large-N_c expansion.

On the experimental side an investigation has been performed at PSI [12], where the form factors have been measured with errors of only a few percent. Older experimental data [13–15] serve as an additional check. Future experiments on the radiative kaon decay will be helpful, as the ratio of the decay widths of the pion and the kaon mode can be predicted theoretically with higher precision than the decay widths individually.

The paper is organized as follows. In Sect. 2 we explain the basic facts of CHPT. The kinematics and the structure of the amplitude and the decay width of the radiative pion decay are presented in Sect. 3. The strong interaction contributions are explained in Sect. 4. Values of the NNLO coupling constants are given. In Sect. 5 we report how the structure of the amplitude is modified by radiative corrections. Apart from that, the treatment of soft photon radiation and the application of the Low theorem is

[a] e-mail: rene.unterdorfer@web.de

explained and the large-N_c form factors used to calculate the radiative corrections to the structure-dependent contributions are introduced. In Sect. 6 our results for the form factors, the radiative corrections and the decay width are presented. Our conclusions are summarized in Sect. 7.

2 Low-energy expansion

The asymptotic states in CHPT are not quarks and gluons but the members of the lightest octet of pseudoscalar mesons[1], the photon and the light leptons. CHPT is a low-energy expansion in the external momenta and masses that should be small compared to the natural scale of chiral symmetry breaking, which is expected to have a value of about 1.2 GeV. The order n of this expansion is indicated by p^n. A squared momentum of a pseudoscalar meson is of $\mathcal{O}(p^2)$. The lowest-order effective Lagrangian is of the form

$$\begin{aligned}\mathcal{L}_{\text{eff}} &= \frac{F^2}{4}\langle u_\mu u^\mu + \chi_+\rangle + e^2F^4 Z\langle UQ_{\rm L}^{\rm em}U^\dagger Q_{\rm R}^{\rm em}\rangle \\ &\quad -\frac{1}{4}F_{\mu\nu}F^{\mu\nu} + \sum_\ell \left[\bar{\ell}(\mathrm{i}\partial\!\!\!/ + e A\!\!\!/ - m_\ell)\ell + \overline{\nu_{\ell\mathrm{L}}}\mathrm{i}\partial\!\!\!/\nu_{\ell\mathrm{L}}\right],\end{aligned} \tag{1}$$

with

$$\begin{aligned} u_\mu &= \mathrm{i}\left[u^\dagger(\partial_\mu - \mathrm{i}r_\mu)u - u(\partial_\mu - \mathrm{i}l_\mu)u^\dagger\right], \\ \chi_\pm &= u^\dagger\chi u^\dagger \pm u\chi^\dagger u .\end{aligned} \tag{2}$$

The pseudoscalar mesons are collected in a matrix u:

$$\begin{aligned} u &= \exp\left(\frac{\mathrm{i}\Phi}{\sqrt{2}F}\right), \quad U = u^2, \\ \Phi &= \begin{pmatrix} \frac{\pi^0}{\sqrt{2}} + \frac{1}{\sqrt{6}}\eta_8 & \pi^+ & K^+ \\ \pi^- & -\frac{\pi^0}{\sqrt{2}} + \frac{1}{\sqrt{6}}\eta_8 & K^0 \\ K^- & \bar{K}^0 & -\frac{2}{\sqrt{6}}\eta_8 \end{pmatrix}. \end{aligned} \tag{3}$$

The symbol $\langle\,\rangle$ stands for the trace in three-dimensional flavor space. In order to introduce masses, the external field χ is set equal to an expression proportional to the quark mass matrix from now on:

$$\chi = 2B_0 \begin{pmatrix} m_u & 0 & 0 \\ 0 & m_d & 0 \\ 0 & 0 & m_s \end{pmatrix}. \tag{4}$$

By adding terms determined via gauge symmetry to the external fields $\tilde{l}_\mu$ and $\tilde{r}_\mu$ of the purely mesonic case the coupling of the photon A_μ and the leptons ℓ and ν_ℓ to the pseudoscalar mesons is fixed.

$$\begin{aligned} l_\mu &= \tilde{l}_\mu - eQ_{\rm L}^{\rm em}A_\mu + \sum_\ell(\bar{\ell}\gamma_\mu\nu_{\ell\mathrm{L}}Q_{\rm L}^{\rm w} + \overline{\nu_{\ell\mathrm{L}}}\gamma_\mu\ell Q_{\rm L}^{\rm w\dagger}), \\ r_\mu &= \tilde{r}_\mu - eQ_{\rm R}^{\rm em}A_\mu . \end{aligned} \tag{5}$$

As the electroweak interactions break chiral symmetry, the spurion matrices $Q_{\rm L,R}^{\rm em}$, $Q_{\rm L}^{\rm w}$ can be equated with the following expressions:

$$\begin{aligned} Q_{\rm L,R}^{\rm em} &= \begin{pmatrix} 2/3 & 0 & 0 \\ 0 & -1/3 & 0 \\ 0 & 0 & -1/3 \end{pmatrix}, \\ Q_{\rm L}^{\rm w} &= -2\sqrt{2}G_{\rm F}\begin{pmatrix} 0 & V_{ud} & V_{us} \\ 0 & 0 & 0 \\ 0 & 0 & 0 \end{pmatrix}. \end{aligned} \tag{6}$$

Every term in the Lagrangian (except kinetic terms) is multiplied with a coupling constant. The constant F in (1) is identified with the pion decay constant in the chiral limit without electroweak interactions. In the same limit the constant B_0 can be related to the quark condensate. Z dominates the pion electromagnetic mass difference. We use the SU(3) formalism in this work, because information from processes involving strange quarks is needed to determine some of the coupling constants.

The lowest-order Lagrangian is not enough to make connection with experiment. Higher orders have to be included. At every order the Lagrangian contains all terms that respect the symmetries. In [6] the SU(3) Lagrangian was presented to $\mathcal{O}(p^4)$ considering also the Wess–Zumino–Witten functional [16, 17]. Here and in the following only the terms relevant for our calculation are shown:

$$\begin{aligned} \mathcal{L}_{p^4} &= L_1\langle u_\mu u^\mu\rangle^2 + L_2\langle u_\mu u_\nu\rangle\langle u^\mu u^\nu\rangle + L_3\langle u_\mu u^\mu u_\nu u^\nu\rangle \\ &\quad - \mathrm{i}L_9\langle f_+^{\mu\nu}u_\mu u_\nu\rangle + \frac{L_{10}}{4}\langle f_{+\mu\nu}f_+^{\mu\nu} - f_{-\mu\nu}f_-^{\mu\nu}\rangle \\ &\quad - \frac{\mathrm{i}}{16\pi^2}\varepsilon^{\mu\nu\alpha\beta}\Big\langle \Sigma_\mu^L U^\dagger\partial_\nu r_\alpha U l_\beta - \Sigma_\mu^R U\partial_\nu l_\alpha U^\dagger r_\beta \\ &\quad + \Sigma_\mu^L l_\nu\partial_\alpha l_\beta + \Sigma_\mu^L\partial_\nu l_\alpha l_\beta - \mathrm{i}\Sigma_\mu^L\Sigma_\nu^L\Sigma_\alpha^L l_\beta \\ &\quad + \mathrm{i}\Sigma_\mu^R\Sigma_\nu^R\Sigma_\alpha^R l_\beta + \frac{3\mathrm{i}}{2}\Sigma_\mu^L(U^\dagger r_\nu U + l_\nu)\langle[v_\alpha, v_\beta]\rangle\Big\rangle \\ &\quad + \ldots, \end{aligned} \tag{7}$$

where

$$\begin{aligned} f_\pm^{\mu\nu} &= uF_{\rm L}^{\mu\nu}u^\dagger \pm u^\dagger F_{\rm R}^{\mu\nu}u, \\ F_{\rm L}^{\mu\nu} &= \partial^\mu l^\nu - \partial^\nu l^\mu - \mathrm{i}[l^\mu, l^\nu], \\ F_{\rm R}^{\mu\nu} &= \partial^\mu r^\nu - \partial^\nu r^\mu - \mathrm{i}[r^\mu, r^\nu], \\ \Sigma_\mu^L &= U^\dagger\partial_\mu U, \quad \Sigma_\mu^R = U\partial_\mu U^\dagger . \end{aligned} \tag{8}$$

To $\mathcal{O}(p^6)$ one has [19–21]

$$\begin{aligned} \mathcal{L}_{p^6} &= C_{12}\langle\chi_+ h_{\mu\nu}h^{\mu\nu}\rangle + C_{13}\langle\chi_+\rangle\langle h_{\mu\nu}h^{\mu\nu}\rangle \\ &\quad + C_{61}\langle\chi_+ f_{+\mu\nu}f_+^{\mu\nu}\rangle + C_{62}\langle\chi_+\rangle\langle f_{+\mu\nu}f_+^{\mu\nu}\rangle \\ &\quad + \mathrm{i}C_{63}\langle f_{+\mu\nu}\{\chi_+, u^\mu u^\nu\}\rangle + \mathrm{i}C_{64}\langle\chi_+\rangle\langle f_{+\mu\nu}u^\mu u^\nu\rangle \\ &\quad + \mathrm{i}C_{65}\langle f_{+\mu\nu}u^\mu\chi_+ u^\nu\rangle + \mathrm{i}C_{78}\langle f_{+\mu\nu}\left[f_-^{\nu\rho}, h_\rho^\mu\right]\rangle \\ &\quad + C_{80}\langle\chi_+ f_{-\mu\nu}f_-^{\mu\nu}\rangle + C_{81}\langle\chi_+\rangle\langle f_{-\mu\nu}f_-^{\mu\nu}\rangle \\ &\quad + C_{82}\langle f_{+\mu\nu}\left[f_-^{\mu\nu}, \chi_-\right]\rangle + C_{87}\langle\nabla_\rho f_{-\mu\nu}\nabla^\rho f_-^{\mu\nu}\rangle \\ &\quad + \mathrm{i}C_{88}\langle\nabla_\rho f_{+\mu\nu}[h^{\mu\rho}, u^\nu]\rangle \\ &\quad + \mathrm{i}C_7^W\varepsilon^{\mu\nu\alpha\beta}\langle\chi_- f_{+\mu\nu}f_{+\alpha\beta}\rangle \\ &\quad + \mathrm{i}C_{11}^W\varepsilon^{\mu\nu\alpha\beta}\langle\chi_-[f_{+\mu\nu}, f_{-\alpha\beta}]\rangle \\ &\quad + C_{22}^W\varepsilon^{\mu\nu\alpha\beta}\langle u_\mu\{\nabla_\gamma f_{+\gamma\nu}, f_{+\alpha\beta}\}\rangle + \ldots, \end{aligned} \tag{9}$$

[1] Other hadrons like the baryons can also be incorporated.

with

$$h_{\mu\nu} = \nabla_\mu u_\nu + \nabla_\nu u_\mu \,, \quad \nabla_\mu X = \partial_\mu X + [\Gamma_\mu, X] \,,$$
$$\Gamma_\mu = \frac{1}{2}[u^\dagger, \partial_\mu u] - \frac{1}{2}\mathrm{i}u^\dagger r_\mu u - \frac{1}{2}\mathrm{i}u l_\mu u^\dagger \,. \quad (10)$$

The Lagrangian of $\mathcal{O}(e^2p^2)$ can be found in [22, 23]. We will not present an $\mathcal{O}(e^2p^4)$ Lagrangian because at this order we use the expression that is of lowest order in the large-N_c expansion.

As CHPT is a quantum field theory, loops have to be taken into account. The primitive degree of divergence of a loop amplitude [18] is equivalent to the chiral dimension. A one-loop Feynman graph including only lowest-order vertices is of $\mathcal{O}(p^4)$ in the purely mesonic case and of $\mathcal{O}(e^2p^2)$ if there is one internal photon propagator. The counterterms used to compensate the ultraviolet divergences of the loop integrals have to be of the same order in the external momenta as the loops. By renormalizing the appropriate coupling constants (e.g. L_9, C_{12}, ...) that appear in the Lagrangian an UV finite amplitude is achieved.

The scale-dependent[2] finite parts of all coupling constants are determined experimentally or estimated by performing resonance exchange calculations. In the large-N_c limit the values of the coupling constants are given by exchange of infinitely narrow resonances. It turns out that at $\mathcal{O}(p^4)$ the values one gets in this approximation agree quite well with the experimental values at a renormalization scale equal to the mass of the ρ particle [24]. This agreement is obtained by using only the lowest-lying vector, axial-vector, scalar and pseudoscalar octets.

In [24] also the constant Z of (1) has been determined. In this case and whenever one wants to calculate a coupling constant of an $\mathcal{O}(e^2p^n)$ Lagrangian resonance, propagators appear in the loop, and the correct momentum dependence of the involved form factors also for high energies [25] is needed. We summarize how this can be achieved in the case of the electromagnetic pion form factor F_e. From (1) and (7) one gets[3]:

$$F_\mathrm{e}(q^2) = 1 + \frac{2L_9^r}{F^2}q^2 + \mathrm{A}_\mathrm{loop} + \mathcal{O}(q^4) \,. \quad (11)$$

At leading order in the $1/N_c$ expansion including the lowest-lying vector resonance with mass M_V we have

$$F_\mathrm{e}(q^2) = 1 + \frac{k_V}{F^2}\frac{q^2}{M_V^2 - q^2} \,. \quad (12)$$

We will identify M_V with the mass of the ρ meson. The chiral loops are of higher order and introduce the width of the ρ [26]. Imposing that the form factor should vanish at infinite momentum transfer due to the Brodsky–Lepage behavior [27, 28], the constant k_V becomes equal to F^2 and

$$F_\mathrm{e}(q^2) = \frac{M_V^2}{M_V^2 - q^2} + \mathcal{O}(1/N_c) \,. \quad (13)$$

[2] The whole amplitude does not depend on the renormalization scale.

[3] The renormalized coupling constants are labeled with an r.

Therefore, one concludes

$$L_9^r(M_V^2) = \frac{F^2}{2M_V^2} \,. \quad (14)$$

The resonance Lagrangian that leads to a pion form factor with the correct low- and high-energy behavior to the order indicated in (11) and (13) is of the form [25]

$$\mathcal{L}_\mathrm{res} = -\frac{1}{2}\langle \nabla^\lambda V_{\lambda\mu} \nabla_\nu V^{\nu\mu} - \frac{M_V^2}{2} V_{\mu\nu} V^{\mu\nu} \rangle$$
$$+ \frac{F_V}{2\sqrt{2}}\langle V_{\mu\nu} f_+^{\mu\nu} \rangle + \frac{\mathrm{i}G_V}{\sqrt{2}}\langle V_{\mu\nu} u^\mu u^\nu \rangle, \quad (15)$$

with the high-energy condition $F_V G_V = F^2$. The vector mesons are described by antisymmetric tensor fields $V_{\mu\nu} = \frac{1}{\sqrt{2}}\sum_{i=1}^{8} \lambda_i V_{\mu\nu}^i$. To $\mathcal{O}(p^4)$, this formalism is equivalent to the more familiar notation with vector fields if one introduces explicit local terms [25].

3 General structure of amplitude and decay width

The amplitude of $\pi^+(p) \to e^+(p_e)\nu(p_\nu)\gamma(k)$ has the following structure [29]:

$$M_0 = -\mathrm{i}eG_\mathrm{F}V_{ud}^*\epsilon_\mu^*\{F_\pi L^\mu - H^{\mu\nu}l_\nu\} \,, \quad (16)$$

with

$$L^\mu = m_e \bar{u}(p_\nu)(1+\gamma_5)\left(\frac{p^\mu}{p\cdot k} - \frac{2p_e^\mu + \not{k}\gamma^\mu}{2p_e\cdot k}\right)v(p_e) \,,$$
$$H^{\mu\nu} = -\frac{\mathrm{i}}{\sqrt{2}m_{\pi^+}}\left(F_V(p_w^2)\epsilon^{\mu\nu\alpha\beta}k_\alpha p_\beta\right.$$
$$\left. - F_A(p_w^2)(k\cdot p g^{\mu\nu} - p^\mu k^\nu)\right) \,,$$
$$l^\mu = \bar{u}(p_\nu)\gamma^\mu(1-\gamma_5)v(p_e), \quad p_w = p_e + p_\nu \,, \quad (17)$$

where F_π is the physical pion decay constant. One distinguishes between the inner Bremsstrahlung (IB) contribution and the structure-dependent (SD) part. The first is given by the term with L_μ and corresponds to the radiation of a pointlike pion and positron. The latter contains the two structure functions $F_V(p_w^2)$ and $F_A(p_w^2)$ including the hadronic contributions.

In the process $\pi \to e\nu\gamma$ the IB part is helicity suppressed, allowing the detection of the structure-dependent terms. The IB contribution diverges if the photon energy goes to zero. This divergence is canceled in the total rate by loop corrections to the decay $\pi \to e\nu$ implying virtual photons. In experiments usually an energy cut is applied. Only photons above a certain energy are detected.

Whereas the IB part is completely determined by the Low theorem [30] the structure-dependent part reflects the influence of QCD on this decay. The form factors F_V and F_A in the chiral expansion are given to $\mathcal{O}(p^4)$ by

$$F_V = \frac{m_{\pi^+}}{F_\pi}\frac{1}{4\sqrt{2}\pi^2} = 0.027 \pm 0.003 \,, \quad (18)$$

$$F_A = m_{\pi^+}\frac{4\sqrt{2}(L_9^r + L_{10}^r)}{F_\pi} = 0.010 \pm 0.004 \,. \quad (19)$$

They include a mass m_{π^+} that is of no physical meaning and drops out in the amplitude (see (17)). At higher orders and by including radiative corrections, the form factors get a momentum dependence.

The importance of the different contributions can be seen from the differential rate (here normalized to the non-radiative mode):

$$\begin{aligned}\frac{\mathrm{d}\Gamma_{e\gamma\nu}}{\mathrm{d}x\,\mathrm{d}y}\Big/\left(\frac{\alpha}{2\pi}\Gamma_{e\nu}\right) &= \mathrm{IB}\,(x,y)+\left(\frac{F_V m_\pi^2}{2\sqrt{2}F_\pi m_e}\right)^2\\ &\times\left[(1+\gamma)^2\,\mathrm{SD}^+\,(x,y)+(1-\gamma)^2\,\mathrm{SD}^-\,(x,y)\right]\\ &+\left(\frac{F_V m_\pi}{\sqrt{2}F_\pi}\right)\left[(1+\gamma)\,S^+_{\mathrm{int}}\,(x,y)+(1-\gamma)\,S^-_{\mathrm{int}}\,(x,y)\right],\end{aligned} \tag{20}$$

with

$$\gamma = F_A/F_V\,. \tag{21}$$

IB, $\mathrm{SD}^\pm$ and $S^\pm_{\mathrm{int}}$ are functions of the two kinematic variables $x=2p\cdot k/m_\pi^2$ and $y=2p\cdot p_e/m_\pi^2$. For $m_e/m_\pi=0$ one has

$$\begin{aligned}\mathrm{IB}(x,y) &= \frac{(1-y)((1+(1-x)^2)}{x^2(x+y-1)}\,,\\ \mathrm{SD}^+(x,y) &= (1-x)(x+y-1)^2\,,\\ \mathrm{SD}^-(x,y) &= (1-x)(1-y)^2\,.\end{aligned} \tag{22}$$

In (20) the terms including $\mathrm{SD}^\pm$ dominate over those with $S^\pm_{\mathrm{int}}$ because of the additional factor m_π^2/m_e^2. When $x+y$ goes to 1 the function $\mathrm{IB}(x,y)$ diverges. $\mathrm{SD}^+(x,y)$ reaches its maximum at $x=2/3$, $y=1$ and $\mathrm{SD}^-(x,y)$ at $x=2/3$, $y=1/3$ (i.e. $x+y=1$). One can define an angle between the positron and photon momenta:

$$\sin^2\frac{\theta_{e\gamma}}{2}=\frac{x+y-1}{xy}\,. \tag{23}$$

For $\theta_{e\gamma}=0$ the function $\mathrm{IB}(x,y)$ goes to infinity and $\mathrm{SD}^-(x,y)$ has its maximum, whereas $\mathrm{SD}^+(x,y)$ has its maximum for $\theta_{e\gamma}=\pi$. Therefore an experiment performed in the region near $\theta_{e\gamma}=\pi$ is sensitive to $(1+\gamma)^2$. It is difficult to distinguish experimentally between the terms proportional to IB and SD^-.

In the standard model weak transitions are described by $V-A$ interactions. New physics could lead to tensor interactions of the form

$$T=\mathrm{i}\frac{eG_{\mathrm{F}}V_{ud}^*}{\sqrt{2}}\epsilon^*_\mu k_\nu F_T\bar{u}(p_\nu)\sigma^{\mu\nu}(1+\gamma^5)v(p_e)\,. \tag{24}$$

Radiative corrections generate an induced tensorial form factor as described in Sect. 5.

4 Contributions due to the strong interaction

The form factors F_V and F_A have been calculated up to $\mathcal{O}(p^6)$ for the chiral group SU(2) in [9] and for SU(3) in [10]. The momentum dependence of the form factors starts at $\mathcal{O}(p^6)$. We will use the SU(3) result, which is in the isospin limit of the following form:

$$\begin{aligned}F_V(p_w^2) &= \frac{m_{\pi^+}}{4\sqrt{2}\pi^2F_\pi}\left\{1-\frac{256}{3}\pi^2m_\pi^2C_7^{Wr}+\frac{64}{3}\pi^2p_w^2C_{22}^{Wr}\right.\\ &\quad+\frac{1}{32\pi^2F_\pi^2}\left[\frac{10}{9}p_w^2-\frac{1}{3}p_w^2\ln\frac{m_\pi^2}{M_\rho^2}\right.\\ &\quad\left.\left.+\frac{4}{3}G(p_w^2/m_\pi^2,m_\pi^2)\right]\right\},\end{aligned} \tag{25}$$

with

$$G(z,m^2)=m^2\left(1-\frac{z}{4}\right)\sqrt{\frac{z-4}{z}}\ln\frac{\sqrt{z-4}+\sqrt{z}}{\sqrt{z-4}-\sqrt{z}}-2m^2 \tag{26}$$

and

$$\begin{aligned}F_A(p_w^2) &= \frac{4\sqrt{2}m_{\pi^+}}{F_\pi}\,(L_9^r+L_{10}^r)\\ &\quad+\frac{m_{\pi^+}}{F_\pi^3}\left\{\frac{1}{\sqrt{2}\pi^2}\left[(-2L_1^r+L_2^r)m_\pi^2\ln\left(\frac{m_\pi^2}{M_\rho^2}\right)\right.\right.\\ &\quad-\left(\frac{1}{2}L_3^r+L_9^r+L_{10}^r\right)\left[m_K^2\ln\left(\frac{m_K^2}{M_\rho^2}\right)\right.\\ &\quad\left.\left.+2m_\pi^2\ln\left(\frac{m_\pi^2}{M_\rho^2}\right)\right]\right]+\frac{m_\pi^2}{6(2\pi)^8}I_2\left(\frac{p_w^2-m_\pi^2}{2m_\pi^2}\right)\\ &\quad-4\sqrt{2}\left[4m_K^2(6C_{13}^r-2C_{62}^r+C_{64}^r+2C_{81}^r)\right.\\ &\quad+2m_\pi^2(6C_{12}^r+6C_{13}^r-2C_{61}^r-2C_{62}^r\\ &\quad+2C_{63}^r+C_{64}^r+C_{65}^r-C_{78}^r\\ &\quad+2C_{80}^r+2C_{81}^r-2C_{82}^r+C_{87}^r)\\ &\quad\left.\left.-\frac{p_w^2-m_\pi^2}{2}(2C_{78}^r-4C_{87}^r+C_{88}^r)\right]\right\}.\end{aligned} \tag{27}$$

All coupling constants are taken at a scale equal to the ρ mass. For the two-loop integral I_2 in (27) the numerical approximation given in [10] is used:

$$I_2(z)=44.5z-10\,304.2\,. \tag{28}$$

The renormalized low-energy constants C_i^{Wr} and C_i^r have to be determined by the use of large-N_c QCD or experimental data. Values for C_7^W and C_{22}^W can be obtained via the conserved-vector-current hypothesis[4] with the help of experimental data [1] on the decays $\pi^0\to\gamma\gamma$ and $\pi^0\to\gamma e^+e^-$. We have

$$|F_{V_{\mathrm{exp}}}^{\pi^0\to\gamma\gamma}(0)|=\frac{1}{\alpha}\sqrt{\frac{2\Gamma(\pi^0\to\gamma\gamma)}{\pi m_{\pi_0}}}=0.0262\pm0.0005\,. \tag{29}$$

The slope parameter of $F_{V_{\mathrm{exp}}}^{\pi^0\to\gamma\gamma}$ is given by

$$a_\pi^{\mathrm{exp}}=0.032\pm0.004\,. \tag{30}$$

[4] The relation that leads to (29) and (30) is reproduced within CHPT if one neglects the kaon loops in case of the decay $\pi^0\to\gamma e^+e^-$.

One gets the following values for the low-energy constants in (25):

$$C_7^{Wr}(M_\rho) = (0.1 \pm 1.2) \times 10^{-9}\,\mathrm{MeV}^{-2}\,,$$
$$C_{22}^{Wr}(M_\rho) = (5.4 \pm 0.8) \times 10^{-9}\,\mathrm{MeV}^{-2}\,. \qquad (31)$$

In [31] the constant C_{12} has been fixed by taking into account the exchange of scalar resonances. The constant C_{61} can be determined with the help of experiments on τ-decays by considering the correlator of two vector currents and using finite-energy sum rule techniques [32, 33]. The combination $2C_{63} - C_{65}$ also appears in the expression for the electromagnetic K_0 charge radius [34, 35] that has been measured [36, 37]. In [38] a large-N_c expression for the correlator of vector, axial-vector and pseudoscalar currents with the correct high-energy behavior fixed by the operator product expansion is used to determine amongst others the low-energy constants C_{78}, C_{82}, C_{87} and C_{88}. The contribution to C_{82} with three propagating resonances is not constrained by the high-energy behavior and will be neglected. The constant C_{80} is fixed with the help of mass and decay constant differences of the a_1 and K_1 particles following an idea presented in [33] for vector mesons (see Appendix C). The situation in the case of axial-vector mesons is more complicated as the states with the quantum numbers $J^{PC} = 1^{++}$ and 1^{+-} mix. The other constants C_{13}, C_{62}, C_{64}, and C_{81} are set zero as resonance exchange does not contribute in this case [39].

In Table 1 the values of the constants C_i at the ρ mass and the information needed for their determination are shown.

The best procedure to get precise values for $F_V(0)$ and for the slope of this form factor is to take the values obtained in the isospin limit via the conserved-vector-current hypothesis (see (29) and (30)) and to add/subtract the theoretical predictions for the isospin breaking (ISB) contributions. The latter are proportional to $m_u - m_d$, e^2 and $m_{\pi^+}^2 - m_{\pi^0}^2$. We have

$$F_V = F_{V_{\mathrm{exp}}}^{\pi^0\to\gamma\gamma} - F_{V_{\mathrm{ISB}}}^{\pi^0\to\gamma\gamma} + F_{V_{\mathrm{ISB}}}^{\pi^+\to e^+\nu\gamma}\,. \qquad (32)$$

In [40] the ISB contribution for $\pi^0 \to \gamma\gamma$ has been calculated with the result

$$F_{V_{\mathrm{ISB}}}^{\pi^0\to\gamma\gamma}(0) = 0.00066 \pm 0.0001 \quad (2.5\% \text{ of } F_{V_{\mathrm{exp}}}^{\pi^0\to\gamma\gamma}(0))\,. \qquad (33)$$

What has to be considered concerning $F_{V_{\mathrm{ISB}}}^{\pi^+\to e^+\nu\gamma}$ are the radiative corrections discussed in Sect. 5 and the following contribution proportional to the additional constant C_{11}^W:

$$F_{V_{m_d-m_u}}^{\pi^+\to e^+\nu\gamma} = \frac{m_\pi}{4\sqrt{2}\pi^2 F_\pi} 256\pi^2 m_\pi^2 \frac{m_d - m_u}{m_d + m_u} C_{11}^W\,. \qquad (34)$$

From experimental data [41] on $K^+ \to \ell^+\nu\gamma$ one gets[5] $C_{11}^{Wr}(M_\rho) = (0.68 \pm 0.21) \times 10^{-9}\,\mathrm{MeV}^{-2}$, which leads to $F_{V_{m_d-m_u}}^{\pi^+\to e^+\nu\gamma} = 0.00025 \pm 0.00009$ (0.9% of $F_{V_{\mathrm{exp}}}^{\pi^0\to\gamma\gamma}(0)$). Numerical results for the form factors $F_{V,A}^{\pi^+\to e^+\nu\gamma}$ can be found in Sect. 6.

[5] We have assumed that the $\mathcal{O}(p^6)$ contribution is smaller than the $\mathcal{O}(p^4)$ part.

Table 1. Values of the coupling constants appearing in (27) and the source of information used to fix them

$C_i^r(M_\rho)$	Value $[10^{-5}]$	Source
C_{12}^r	-0.6 ± 0.3	scalar resonance exchange
C_{13}^r	0 ± 0.2	resonance exchange
C_{61}^r	1.0 ± 0.3	τ decays, $\langle VV \rangle$ correlator
C_{62}^r	0 ± 0.2	resonance exchange
$2C_{63}^r - C_{65}^r$	1.8 ± 0.7	K_0 charge radius
C_{64}^r	0 ± 0.2	resonance exchange
C_{78}^r	10.0 ± 3.0	resonance exchange
C_{80}^r	1.8 ± 0.4	a_1, K_1 differences
C_{81}^r	0 ± 0.2	resonance exchange
C_{82}^r	-3.5 ± 1.0	resonance exchange
C_{87}^r	3.6 ± 1.0	resonance exchange
C_{88}^r	-3.5 ± 1.0	resonance exchange

5 Radiative corrections

The amplitude including radiative corrections contains additional terms compared to (17) and is of the form

$$\begin{aligned} M &= -\mathrm{i} G_{\mathrm{F}} e V_{ud}^* \epsilon_\mu^* \{F_\pi L^\mu F_{\mathrm{IB}}(x,y) - H^{\mu\nu} l_\nu\} \\ &\quad + T(x,y)\,, \\ H^{\mu\nu} &= -\frac{\mathrm{i}}{\sqrt{2} m_\pi} \big(\epsilon^{\mu\nu\alpha\beta} V_{\alpha\beta}(x,y) \\ &\quad - F_A(x,y)(k\cdot p g^{\mu\nu} - p^\mu k^\nu) \\ &\quad - \hat{F}_A(x,y)(k\cdot p_l g^{\mu\nu} - p_l^\mu k^\nu)\big)\,, \end{aligned} \qquad (35)$$

where $V_{\alpha\beta}(x,y)$ has a tensor structure more complicated than $F_V(q^2)k_\alpha p_\beta$ and one can distinguish between two different axial-vector form factors. As mentioned above, the radiative corrections generate in addition an induced tensorial form factor $T(x,y)$ that is very small, i.e. 0.5%–1.5% of the IB part of the differential branching ratio depending on x and y. To $\mathcal{O}(e^2p^2)$ there is no contribution to $V_{\alpha\beta}(x,y)$ and the contributions to $F_A(x,y)$ and $\hat{F}_A(x,y)$ turn out to be proportional to m_e^2/m_π^2 and can be neglected. Therefore, the lowest-order radiative corrections (including also the induced tensorial form factor) can be regarded as corrections to the IB part.

The squared amplitude $|M_0|^2$ receives radiative corrections due to virtual loop photons Δ_{V} and additional soft real photons Δ_{S}:

$$\sum_{\mathrm{spin}} |M|^2 = \sum_{\mathrm{spin}} |M_0|^2 \left(1 + \frac{\alpha}{\pi}(\Delta_{\mathrm{V}} + \Delta_{\mathrm{S}})\right)\,, \qquad (36)$$

$$\Delta_{\mathrm{S}} = -\frac{1}{2\pi}\int \frac{\mathrm{d}^3 k_1}{2\omega_1}\left(\frac{p}{(k_1 p)} - \frac{p_e}{(k_1 p_e)}\right)^2\Bigg|_{\omega_1 < \Delta E}\,, \qquad (37)$$

where ω_1 is equal to $\sqrt{\mathbf{k}_1^2+\lambda^2}$ with a photon mass λ, introduced to deal with the infrared divergences, and ΔE is the maximally allowed energy of the soft photon. The infrared divergent terms given by

$$\begin{aligned}\Delta_{\mathrm{S}} &= \left(\ln\left(\frac{y^2 m_\pi^2}{m_e^2}\right) - 2\right)\ln\left(\frac{2\Delta E}{\lambda}\right) + \dots \\ \Delta_{\mathrm{V}} &= -\left(\ln\left(\frac{y^2 m_\pi^2}{m_e^2}\right) - 2\right)\ln\left(\frac{m_\pi}{\lambda}\right) + \dots \end{aligned} \tag{38}$$

cancel each other. The Feynman diagrams with a virtual loop photon are shown in Fig. 1.

The constant part of $F_{\mathrm{IB}}(x,y)$ is obtained from the amplitude of $\pi^+ \to e^+\nu$ via the Low theorem:

$$\begin{aligned}F_{\mathrm{IB}}(x,y) = 1 + e^2\Bigg(&\frac{4}{3}K_1 + \frac{4}{3}K_2 + \frac{10}{9}K_5 + \frac{10}{9}K_6 \\ &+ 2K_{12} - \frac{2}{3}X_1 - 2X_2 + 2X_3 \\ &- \frac{1}{2}X_6 + A_{\mathrm{loop}}(x,y)\Bigg)\,. \end{aligned} \tag{39}$$

The K_i and X_i are coupling constants of the $\mathcal{O}(e^2p^2)$ Lagrangian. By use of experimental data on the decay $\pi^+ \to \mu^+\nu$ no unknown low-energy constants remain to $\mathcal{O}(e^2p^2)$.

As the form factors F_V and F_A have been determined up to $\mathcal{O}(p^6)$ it makes sense to calculate also the radiative corrections of $\mathcal{O}(e^2p^4)$. In Table 2 we show the even-intrinsic-parity $\mathcal{O}(p^4)$ vertices that are needed. The axial field J^+ is always replaced by $2\sqrt{2}G_{\mathrm{F}}V_{ud}^* e^+\gamma_\mu\nu_{e_{\mathrm{L}}}$. The odd-intrinsic-parity vertices can be derived from (7). We will work at lowest order in the large-N_c expansion, therefore we will not include purely mesonic loops in our calculation. In addition one has to consider counterterms of $\mathcal{O}(e^2p^4)$. But as the coupling constants appearing in these counterterms are unknown, we use large-N_c form factors that include the $\mathcal{O}(p^4)$ vertices and also produce the counterterm contributions as indicated in (12) in the case of the pion form factor. We will restrict ourselves to propagating ρ particles; for the a_1 a momentum independent contracted propagator will be used. By doing this one misses the contributions to the $\mathcal{O}(e^2p^4)$ coupling constants coming from a_1 exchange, which enlarges the error. We also do not consider resonance exchange in the odd-intrinsic-parity sector.

It turns out that one just has to make the following replacements in the vertices in Table 2 in order to get the corresponding form factors obtained by use of the resonance Lagrangian equation (15):

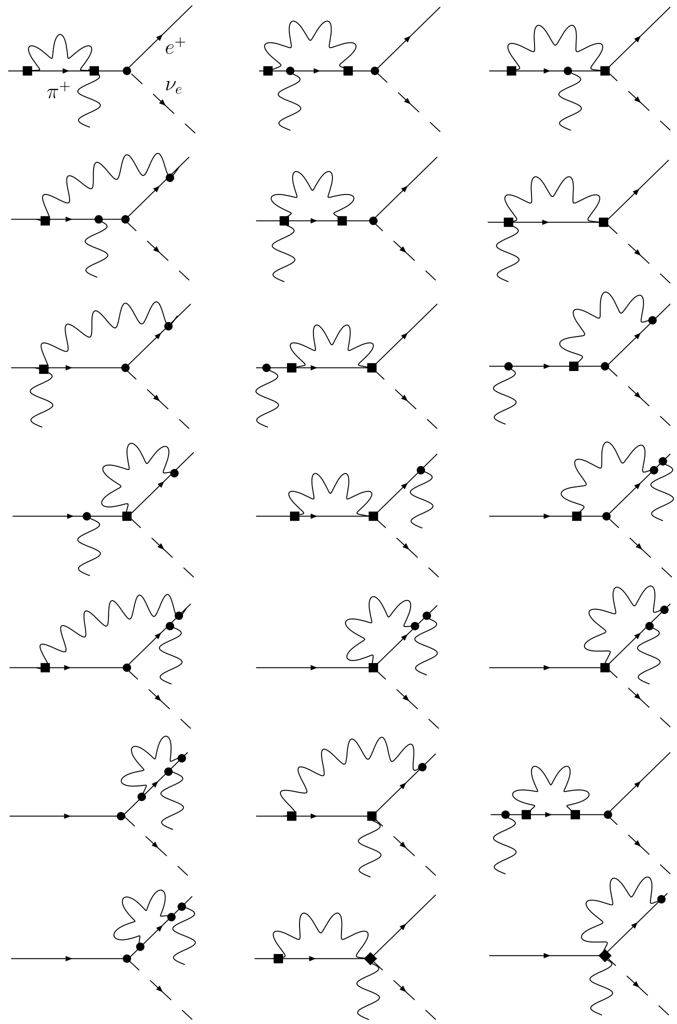

Fig. 1. Feynman diagrams of the virtual radiative corrections. The *dot* is a lowest-order vertex, the *diamond* is an $\mathcal{O}(p^4)$ vertex and the *square* can be an $\mathcal{O}(p^2)$ or an $\mathcal{O}(p^4)$ vertex. Diagrams due to wave-function renormalization are not shown

$$L_9^r \to \frac{F_V G_V}{2(M_\rho^2 - q_i^2)}\,, \quad L_{10}^r \to -\frac{F_V^2}{4(M_\rho^2 - q_i^2)}\,. \tag{40}$$

Here q_i is the momentum of the virtual photon.

The sum of the loop graphs including the large-N_c form factors is UV finite except the graph that contains the

Table 2. Even-intrinsic-parity vertices that are needed to calculate the loop amplitude of $\mathcal{O}(e^2p^4)$

Vertex	$\mathcal{O}(p^4)$ expression
$\pi^+(v)\pi^-(t)\gamma^*(q)$	$\frac{4e}{F^2}\left(q^2\, v\cdot\epsilon - v\cdot q\, q\cdot\epsilon\right)L_9^r$
$\pi^+(v)\pi^-(t)\gamma(q_1)\gamma^*(q_2)$	$\frac{4e^2}{F^2}((\epsilon_1\cdot\epsilon_2\, q_2^2 - \epsilon_1\cdot q_2\, q_2\cdot\epsilon_2)L_9^r + 2(q_1\cdot q_2\,\epsilon_1\cdot\epsilon_2 - q_1\cdot\epsilon_2\,\epsilon_1\cdot q_2)(L_9^r + L_{10}^r))$
$\pi^+(v)\gamma^*(q)J^+(w)$	$-\frac{4ie}{F}((\epsilon_w\cdot\epsilon\, q^2 - \epsilon_w\cdot q\, q\cdot\epsilon)L_9^r + (w\cdot q\,\epsilon_w\cdot\epsilon - w\cdot\epsilon\,\epsilon_w\cdot q)(L_9^r + L_{10}^r))$
$\pi^+(v)\gamma(q_1)\gamma^*(q_2)J^+(w)$	$\frac{4ie^2}{F}(q_2\cdot\epsilon_w\,\epsilon_1\cdot\epsilon_2 - q_2\cdot\epsilon_1\,\epsilon_2\cdot\epsilon_w + q_1\cdot\epsilon_w\,\epsilon_1\cdot\epsilon_2 - q_1\cdot\epsilon_2\,\epsilon_1\cdot\epsilon_w)(L_9^r + L_{10}^r)$

third vertex of Table 2 with an external photon and no loop photon. This divergence is due to the fact that the a_1 propagator has been contracted. With a propagating a_1 in the loop also this graph is finite. So we make the following replacement in order to get a finite result:

$$-\frac{1}{(4\pi)^2}\ln\left(\frac{M_\rho^2}{\mu^2}\right)-\frac{2\mu^{d-4}}{(4\pi)^2}\left(\frac{1}{d-4}-\frac{1}{2}(\ln(4\pi)\right.$$
$$\left.+\Gamma'(1)+1)\right)\to-\frac{1}{(4\pi)^2}\ln\left(\frac{M_\rho^2}{M_{a_1}^2}\right). \quad (41)$$

Related to wave-function renormalization in the $\mathcal{O}(e^2p^4)$ amplitude, there is a term of the form

$$\left(1-\frac{1}{2}e^2(X_6-4K_{12})\right)\times 4\sqrt{2}m_{\pi^+}/\tilde{F}_\pi\,(L_9^r+L_{10}^r), \quad (42)$$

where $\tilde{F}_\pi$ is the physical decay constant, which also includes the $\mathcal{O}(e^2)$ contributions. As shown in (42), we get a short-distance factor of the correct form [42], but it is unrenormalized. Our resonance calculation of the rest of the $\mathcal{O}(e^2p^4)$ amplitude that is finite by itself and valid to lowest order in the large-N_c expansion does not generate the counterterm to renormalize the short-distance factor. One has to perform a two-step matching procedure of CHPT to Fermi theory and to the standard model [42]. We will use the following result [42] for the renormalized short-distance factor:

$$\begin{aligned}S_{\mathrm{EW}}&=1-\frac{1}{2}e^2\left(X_6^r(M_\rho^2)-4K_{12}^r(M_\rho^2)\right)\\&=1-\frac{e^2}{32\pi^2}\left(-8\ln\left(\frac{M_Z}{M_\rho}\right)+\frac{1}{2}\ln\left(\frac{M_{a_1}^2}{M_\rho^2}\right)\right.\\&\qquad\left.-\frac{M_{a_1}^2+3M_\rho^2}{16F^2\pi^2}+\frac{7}{2}\right). \quad (43)\end{aligned}$$

Putting together all contributions (see also Appendix A) and using the physical electron mass, the decay width with radiative corrections up to $\mathcal{O}(e^2p^4)$ is of the form

$$\begin{aligned}\frac{\mathrm{d}\Gamma_{e\gamma\nu}}{\mathrm{d}x\,\mathrm{d}y}&=G_\mathrm{F}^2|V_{ud}|^2\alpha S_{\mathrm{EW}}\\&\times\left\{\frac{m_e^2m_\pi F_\pi^2}{8\pi^2}\mathrm{IB}\,(x,y)\left(1+\frac{\alpha}{\pi}\Delta_{\mathrm{IB}}(x,y)\right)\right.\\&+\frac{F_V^2m_\pi^5}{64\pi^2}\left[(1+\gamma)^2\,\mathrm{SD}^+\,(x,y)\right.\\&\left.\left.+(1-\gamma)^2\,\mathrm{SD}^-\,(x,y)\right]\left(1+\frac{\alpha}{\pi}\Delta_{\mathrm{SD}}(x,y)\right)\right\}. \quad (44)\end{aligned}$$

6 Results

We predict the following form factors of (17) without radiative corrections:

$$\begin{aligned}F_V^{\pi^+\to e^+\nu\gamma}&=0.0262\pm0.0005\\&\quad+(8.72\pm1.09)\times10^{-4}p_w^2/m_\pi^2+\mathcal{O}(p_w^4),\\F_A^{\pi^+\to e^+\nu\gamma}&=0.0106\pm0.0036\\&\quad+(2.03\pm0.65)\times10^{-4}p_w^2/m_\pi^2+\mathcal{O}(p_w^4),\end{aligned} \quad (45)$$

where p_w^2 is equal to $m_\pi^2(1-x)$. Except for the small isospin breaking contributions F_V is determined by the data on the decays $\pi^0\to\gamma\gamma$ and $\pi^0\to\gamma e^+e^-$. The $\mathcal{O}(p^6)$ contribution to $F_A(0)$ is about 15% and very sensitive to the values of the L_i. We have used the set of the L_i given in Appendix B. With the older set of values quoted in [10] the $\mathcal{O}(p^6)$ contribution would be bigger. The relatively large error of $F_A(0)$ is due to the fact that the following sum of coupling constants is not known precisely:

$$L_9^r+L_{10}^r=(1.39\pm0.28)\times10^{-3}. \quad (46)$$

In contrast to [10] we have quoted the values for all of the appearing coupling constants, and updated values are used. This is the reason for the difference of a few percent

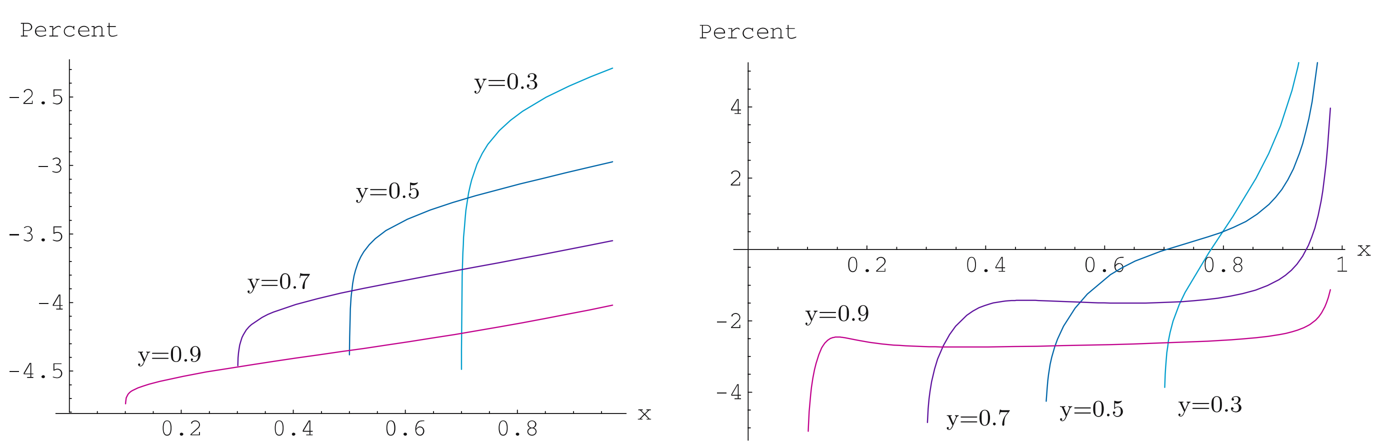

Fig. 2. The relative size of the radiative corrections to the $\mathcal{O}(e^2p^2)$ contribution (*left figure*) and to the $\mathcal{O}(e^2p^4)$ part (*right figure*) for $y=0.3$, $y=0.5$, $y=0.7$ and $y=0.9$

Table 3. Theoretical (R_{the}) and measured (R_{exp}) branching ratios for the three indicated phase space regions

$E_{e^+}^{\min}$ (MeV)	$E_\gamma^{\min}$ (MeV)	$\theta_{e\gamma}^{\min}$ (°)	R_{the} ($\times 10^{-8}$)	R_{exp} ($\times 10^{-8}$)
50	50	–	2.58(8)	2.655(58)
10	50	40	14.77(40)	14.59(26)
50	10	40	38.89(90)	37.95(60)

between the theoretical results presented in [10] and in this paper.

In Fig. 2 we show the size of the radiative corrections $\frac{\alpha}{\pi}\Delta_{\mathrm{IB}}$ (left figure) and $\frac{\alpha}{\pi}\Delta_{\mathrm{SD}}$ (right figure) in percent depending on the kinematic variable x for four different choices of y. The first are negative over the whole phase space and smaller than 5%. The latter are between -4% and $+4\%$. The maximally allowed energy of the soft photon ΔE is set equal to 30 MeV. Up to a small difference, which could be due to a misprint, we agree with the result for $\Delta_{\mathrm{IB}}(x,y)$ in [11] under the assumption that in [11] the electron mass without radiative corrections and not the physical electron mass is used. The expression $1+\frac{\alpha}{\pi}\Delta_{\mathrm{IB}}(x,y)$ is used in [11] as an overall factor for the complete decay width and not only for the inner Bremsstrahlung part. This is only correct in the leading logarithmical approximation. But as all the dependence on m_e/m_π cancels in the total decay width in accordance with the Kinoshita–Lee–Nauenberg theorem [43, 44] one needs the CHPT expression to estimate the magnitude of the radiative corrections to the structure-dependent part of the total decay width.

In Table 3 we compare the results for the branching ratios including all contributions with data [12] for experimental cuts indicated by $E_{e^+}^{\min}$, $E_\gamma^{\min}$ and $\theta_{e\gamma}^{\min}$. Our results agree with the experimental data [12].

The fact that the theoretical branching ratio is very sensitive to $L_9^r + L_{10}^r$ allows for a rather precise determination of this sum of coupling constants if one uses the experimental result for the cuts $E_{e^+}^{\min} = 50$ MeV and $E_\gamma^{\min} = 50$ MeV at $\mathcal{O}(p^4)$ (first line) and at $\mathcal{O}(p^6)$ (second line):

$$(L_9^r(M_\rho) + L_{10}^r(M_\rho))^{\mathrm{fit}} = \begin{cases} (1.32 \pm 0.14) \times 10^{-3}, \\ (1.44 \pm 0.08) \times 10^{-3}. \end{cases} \tag{47}$$

This result is in good agreement with the existing theoretical prediction in (46).

7 Conclusions

The radiative pion decay that includes an inner Bremsstrahlung part and a structure-dependent contribution has been reanalyzed. We have calculated the radiative corrections to the structure-dependent part to lowest order in the large-N_c expansion within CHPT for the first time. Explicit values for all of the occurring $\mathcal{O}(p^6)$ coupling constants have been given by using and extending existing results [32–34, 38].

It turns out that the $\mathcal{O}(p^6)$ contribution is about 15%. The radiative corrections are a few percent varying over the phase space. The branching ratio agrees within the errors with the experimental data [12]. There is no need to introduce a tensor interaction to explain the measured differential decay width obtained by the use of the new data set [12]. The CVC hypothesis that relates the vector form factor of the radiative pion decay to the decay $\pi^0 \to \gamma\gamma$ seems to be a good approximation.

The biggest theoretical error comes from the fact that the quite small sum of the coupling constants L_9^r and L_{10}^r is not known with high precision. As a consequence a possible new physics contribution that affects the axial-vector form factor F_A is difficult to detect. Experimental data [12] allow for a precise determination of $L_9^r + L_{10}^r$, which also appears in the radiative kaon decays $K^+ \to e^+\nu_e\gamma$ and $K^+ \to \mu^+\nu_\mu\gamma$ and in Compton scattering $\gamma\pi^+ \to \gamma\pi^+$.

Acknowledgements. We are grateful to Gerhard Ecker, Roland Rosenfelder and Karol Kampf for useful discussions and reading through this manuscript.

Appendix A: Explicit form of corrections Δ_{IB} and Δ_{SD}

The radiative corrections introduced in (44) are of the following form [11]:

$$\begin{aligned}
\Delta_{\mathrm{IB}}(x,y) &= \frac{x(x(y-1)-2y)\ln^2(y)}{4\,(x^2-2x+2)\,(y-1)} \\
&+ \frac{\left((1-y)x^2+2(y-2)x-4y+4\right)\ln(x)\ln(y)}{(x^2-2x+2)\,(y-1)} \\
&+ \frac{x\left(y^2+1\right)\ln(x+y-1)\ln(y)}{(x^2-2x+2)\,(y-1)} + \frac{\ln(y)}{2} \\
&- \frac{x(x+y-1)\left(y^2+xy-2y+x-1\right)\ln^2(x+y-1)}{2\,(x^2-2x+2)\,(x+y-2)^2} \\
&+ \frac{\pi^2\left(-3(y-1)x^2+2\left(y^2+3y-5\right)x-12(y-1)\right)}{12\,(x^2-2x+2)\,(y-1)} \\
&+ \frac{\left((y-1)x^2-2(y-2)x+4(y-1)\right)\ln(1-x)\ln(x)}{2\,(x^2-2x+2)\,(y-1)} \\
&- 2\ln\left(\frac{2\Delta E}{y m_\pi}\right) + \ln\left(\frac{2\Delta E}{y m_\pi}\right)\ln\left(\frac{y^2 m_\pi^2}{m_e^2}\right) \\
&+ \frac{(x-1)x(x+y-1)\ln(x+y-1)}{(x^2-2x+2)\,(x+y-2)} \\
&- \frac{3}{4}\ln\left(\frac{y^2 m_\pi^2}{m_e^2}\right) + \frac{x(-yx+x+2y)\mathrm{Li}_2(1-x)}{2\,(x^2-2x+2)\,(y-1)} \\
&+ \frac{\left((y-1)x^2-2(y-2)x+4(y-1)\right)\mathrm{Li}_2(x)}{2\,(x^2-2x+2)\,(y-1)} \\
&- \frac{x(x+y-1)\mathrm{Li}_2(1-y)}{2\,(x^2-2x+2)} + \frac{x(x+y-1)\mathrm{Li}_2\left(\frac{y-1}{y}\right)}{2\,(x^2-2x+2)} \\
&- \frac{x^2+2}{4\,(x^2-2x+2)} - \frac{3}{4}\ln\left(\frac{M_\rho^2}{m_\pi^2}\right) - C_1 + \frac{1}{2}\,.
\end{aligned} \tag{A.1}$$

ΔE is the maximal energy of the not detected additional soft photon and C_1, which is given by [23]

$$
\begin{aligned}
C_1 = &-4\pi^2 \left(\frac{8}{3} K_1^r + \frac{8}{3} K_2^r + \frac{20}{9} K_5^r + \frac{20}{9} K_6^r + 4K_{12}^r \right. \\
&\left. - \frac{4}{3} X_1^r - 4X_2^r + 4X_3^r - X_6^r \right) - \frac{1}{2} + \ln\left(\frac{M_Z^2}{M_\rho^2}\right) \\
&+ \frac{Z}{4}\left[3 + 2\ln\left(\frac{m_\pi^2}{M_\rho^2}\right) + \ln\left(\frac{m_K^2}{M_\rho^2}\right)\right], \qquad \text{(A.2)}
\end{aligned}
$$

has been defined in [45]. We have

$$
\begin{aligned}
&\Delta_{\mathrm{SD}}(x,y) \\
&= \ln\left(\frac{2\Delta E}{y m_\pi}\right)\left(\ln\left(\frac{y^2 m_\pi^2}{m_e^2}\right) - 2\right) \\
&\quad + \frac{\ln^2(y)}{2} + \frac{3}{4}\ln\left(\frac{y^2 m_\pi^2}{m_e^2}\right) + \mathrm{Li}_2\left(\frac{y-1}{y}\right) \\
&\quad + \left[\frac{3}{2}(x-1)(y-1)^2 \ln(y)\left(32\pi^2 L_9^r + 32\pi^2 L_{10}^r - 1\right)^2\right. \\
&\quad + \frac{4F^2\pi^2(x-1)}{M_{a_1}^2 M_\rho^2} \ln\left(\frac{M_\rho^2}{M_{a_1}^2}\right) \{[x\,(x+2y-2) \\
&\quad + 32\pi^2\left(x^2 + 2(y-1)x + 2(y-1)^2\right)\left(L_9^r + L_{10}^r\right)] \\
&\quad \times \left(M_{a_1}^2 - M_\rho^2\right)\} \\
&\quad + \ln\left(\frac{M_\rho^2}{m_\pi^2}\right)[(x-1) \\
&\quad \times \left(M_{a_1}^2\left(16\pi^2\left(15x^2 + 30(y-1)x + 13(y-1)^2\right)F^2\right.\right. \\
&\quad + \left.\left(25x^2 + 50(y-1)x + 44(y-1)^2\right)M_\rho^2\right) \\
&\quad - 16F^2\pi^2\left(15x^2 + 30(y-1)x + 13(y-1)^2\right)M_\rho^2\big) \\
&\quad + 32\pi^2 L_9^r\left(M_{a_1}^2\left(16\pi^2(x-1)\right.\right. \\
&\quad \times \left(15x^2 + 30(y-1)x + 17(y-1)^2\right)F^2 \\
&\quad + \left(25x^3 + (62y-87)x^2\right. \\
&\quad + \left.\left.2\left(9y^2 - 55y + 46\right)x - 30(y-1)^2\right)M_\rho^2\right) \\
&\quad - 16F^2\pi^2(x-1) \\
&\quad \times \left.\left(15x^2 + 30(y-1)x + 17(y-1)^2\right)M_\rho^2\right) \\
&\quad + 32\pi^2 L_{10}^r(M_{a_1}^2\left(16\pi^2(x-1)\right. \\
&\quad \times \left(15x^2 + 30(y-1)x + 17(y-1)^2\right)F^2 \\
&\quad + \left(25x^3 + (62y-87)x^2\right. \\
&\quad + \left.\left.2\left(9y^2 - 55y + 46\right)x - 30(y-1)^2\right)M_\rho^2\right) \\
&\quad - 16F^2\pi^2(x-1) \\
&\quad \times \left.\left(15x(x+2y-2) + 17(y-1)^2\right)M_\rho^2)\right] \\
&\quad \Big/ \left(12 M_{a_1}^2 M_\rho^2\right) \\
&\quad - \frac{(x-1)}{x^2}\mathrm{Li}_2(1-x) \\
&\quad \times \left(1024\pi^4(x-2)\right. \\
&\quad \times \left(x^2 + 2(y-1)x + 2(y-1)^2\right)L_9^{r2} \\
&\quad + 64\pi^2\left[32\pi^2(x-2)\right. \\
&\quad \times \left(x^2 + 2(y-1)x + 2(y-1)^2\right)L_{10}^r \\
&\quad - \left.x(x+2y-2)\right]L_9^r \\
&\quad + 1024\pi^4(x-2)\left(x^2 + 2(y-1)x + 2(y-1)^2\right)L_{10}^{r2} \\
&\quad - x\left(x^2 + 2(y-1)x + 2(y-1)^2\right) \\
&\quad - \left.64\pi^2 x(x+2y-2)L_{10}^r\right) \\
&\quad - \ln(x)\left[\left(1024\pi^4\left(x^2 + 4x - 4\right)\right.\right. \\
&\quad \times \left(x^2 + 2(y-1)x + 2(y-1)^2\right)L_9^{r2} \\
&\quad + 64\pi^2\left(x\left(x^2 + x - 2\right)(x+2y-2)\right. \\
&\quad + 32\pi^2\left(x^2 + 4x - 4\right) \\
&\quad \times \left.\left(x^2 + 2(y-1)x + 2(y-1)^2\right)L_{10}^r\right)L_9^r \\
&\quad + 1024\pi^4\left(x^2 + 4x - 4\right) \\
&\quad \times \left(x^2 + 2(y-1)x + 2(y-1)^2\right)L_{10}^{r2} \\
&\quad + (x-2)x\left(x^2 + 2(y-1)x + 2(y-1)^2\right) \\
&\quad + \left.\left.64\pi^2 x\left(x^2 + x - 2\right)(x+2y-2)L_{10}^r\right)\right] \Big/ (2x) \\
&\quad + \frac{1}{6}\ln(x+y-1) \\
&\quad \times \left(-2048\pi^4(x-1)\right. \\
&\quad \times \left(3x^2 + 6(y-1)x + 4(y-1)^2\right)L_9^{r2} \\
&\quad - 32\pi^2\left(11x^3 + 28yx^2 - 39x^2 + 4y^2 x\right. \\
&\quad - 42yx + 38x - 10y^2 + 20y \\
&\quad + 128\pi^2(x-1) \\
&\quad \times \left.\left(3x^2 + 6(y-1)x + 4(y-1)^2\right)L_{10}^r - 10\right)L_9^r \\
&\quad - 2048\pi^4(x-1) \\
&\quad \times \left(3x^2 + 6(y-1)x + 4(y-1)^2\right)L_{10}^{r2} \\
&\quad - (x-1)\left(5x^2 + 10(y-1)x + 16(y-1)^2\right) \\
&\quad - 32\pi^2\left(11x^3 + (28y-39)x^2\right. \\
&\quad + \left.\left.(4y^2 - 42y + 38)x - 10(y-1)^2\right)L_{10}^r\right) \\
&\quad + \left\{1024\pi^4(x-1)\right. \\
&\quad \times \left[6\pi^2\left(x^2 + x - 2\right)\left(x^2 + 2(y-1)x + 2(y-1)^2\right)\right. \\
&\quad + x\left(105x^3 + 6(36y-25)x^2 + 2\left(31y^2 + 7y - 38\right)x\right. \\
&\quad + \left.\left.144(y-1)^2\right)\right]L_9^{r2} M_{a_1}^2 M_\rho^2 y^3 \\
&\quad + 1024\pi^4(x-1) \\
&\quad \times \left[6\pi^2\left(x^2 + x - 2\right)\left(x^2 + 2(y-1)x + 2(y-1)^2\right)\right. \\
&\quad + x\left(105x^3 + 6(36y-25)x^2\right. \\
&\quad + \left.\left.2\left(31y^2 + 7y - 38\right)x + 144(y-1)^2\right)\right] \\
&\quad \times L_{10}^{r2} M_{a_1}^2 M_\rho^2 y^3 \\
&\quad - 64\pi^2 x L_{10}^r\left(4F^2\pi^2(x-1)x\left\{\left[3\left(y^3 - 27y + 18\right)x^2\right.\right.\right. \\
&\quad + 6\left(y^4 - y^3 - 27y^2 + 45y - 18\right)x \\
&\quad - \left.(y-1)^2\left(92y^3 + 81y - 54\right)\right]M_{a_1}^2 \\
&\quad + \left[-3\left(5y^3 - 27y + 18\right)x^2\right. \\
&\quad - 6\left(5y^4 - 5y^3 - 27y^2 + 45y - 18\right)x \\
&\quad + \left.\left.(y-1)^2\left(20y^3 + 81y - 54\right)\right]M_\rho^2\right\} \\
&\quad - y^3\left[6\pi^2(x+1)(x+2y-2)(x-1)^2\right. \\
&\quad + x\left(96x^3 + 4(56y-71)x^2\right. \\
&\quad + \left(120y^2 - 439y + 283\right)x
\end{aligned}
$$

$$
\begin{aligned}
&- \ 164y^2+259y-95)\big]\, M_{a_1}^2 M_\rho^2\big)\\
&-(x-1)x\left(8F^2\pi^2 x\left\{\left[3\left(y^3-27y+18\right)x^2\right.\right.\right.\\
&+6\left(y^4-y^3-27y^2+45y-18\right)x\\
&+\left.(y-1)^2\left(98y^3-81y+54\right)\right] M_{a_1}^2\\
&+\left[-3\left(5y^3-27y+18\right)x^2\right.\\
&-6\left(5y^4-5y^3-27y^2+45y-18\right)x\\
&-\left.\ (y-1)^2\left(50y^3-81y+54\right)\right] M_\rho^2\Big\}\\
&-y^3\left\{6\pi^2(x-1)\left(x^2+2(y-1)x+2(y-1)^2\right)\right.\\
&+x\left[87x^2+6(25y-24)x\right.\\
&+\left.\left.\ 4\left(32y^2-61y+29\right)\right]\right\} M_{a_1}^2 M_\rho^2\Big)\\
&+64\pi^2 L_9^r\left[32\pi^2(x-1)\right.\\
&\times\left[6\pi^2(x^2+x-2)\left(x^2+2(y-1)x+2(y-1)^2\right)\right.\\
&+x\left(105x^3+6(36y-25)x^2\right.\\
&+\left.\left.\ 2\left(31y^2+7y-38\right)x+144(y-1)^2\right)\right] L_{10}^r M_{a_1}^2 M_\rho^2 y^3\\
&+x\left(y^3\left[6\pi^2(x+1)(x+2y-2)(x-1)^2\right.\right.\\
&+x\left(96x^3+4(56y-71)x^2\right.\\
&+\left.\left.\ \left(120y^2-439y+283\right)x-164y^2+259y-95\right)\right]\\
&\times M_{a_1}^2 M_\rho^2\\
&-4F^2\pi^2(x-1)x\left[\left[3\left(y^3-27y+18\right)x^2\right.\right.\\
&+6\left(y^4-y^3-27y^2+45y-18\right)x\\
&-\left.(y-1)^2\left(92y^3+81y-54\right)\right] M_{a_1}^2\\
&+\left[-3\left(5y^3-27y+18\right)x^2\right.\\
&-6\left(5y^4-5y^3-27y^2+45y-18\right)x\\
&+\left.\left.\ (y-1)^2\left(20y^3+81y-54\right)\right] M_\rho^2\right]\Big)\Big]\Big\}\\
&\Big/\left(36x^2y^3 M_{a_1}^2 M_\rho^2\right)\Big]\\
&\Big/\Big((y-1)^2\left(32\pi^2\left(L_9^r+L_{10}^r\right)-1\right)^2\\
&+(x+y-1)^2\left(32\pi^2\left(L_9^r+L_{10}^r\right)+1\right)^2\Big)\Big/(1-x)\\
&-\frac{16\pi^2}{9}\left(6(K_1^r+K_2^r)+5\left(K_5^r+K_6^r\right)+9K_{12}^r\right). \qquad \text{(A.3)}
\end{aligned}
$$

Appendix B: Numerical input

In this appendix we collect the numerical values of coupling constants and masses used in this article that have not already been explained before.

Masses [1]

$M_\rho = 775\,\text{MeV}$, $M_{a_1} = \sqrt{2}M_\rho$,
$m_{\pi^0} = 134.977\,\text{MeV}$, $m_{\pi^+} = 139.570\,\text{MeV}$,
$m_\pi = (m_{\pi^0}+m_{\pi^+})/2$.

Chiral low-energy constants [42, 46–48]

$F = 87.7\pm0.3\,\text{MeV}$, $F_\pi = 92.2\pm0.3\,\text{MeV}$,
$L_1^r = (0.43\pm0.12)\times10^{-3}$, $L_2^r = (0.73\pm0.12)\times10^{-3}$,
$L_3^r = (-2.53\pm0.37)\times10^{-3}$, $L_9^r = (6.49\pm0.20)\times10^{-3}$,
$L_{10}^r = (-5.10\pm0.20)\times10^{-3}$, $K_1^r = (-2.7\pm0.9)\times10^{-3}$,
$K_2^r = (0.7\pm0.3)\times10^{-3}$, $K_5^r = (11.6\pm3.5)\times10^{-3}$,
$K_6^r = (2.8\pm0.9)\times10^{-3}$, $K_{12}^r = (-4.2\pm1.5)\times10^{-3}$,
$C_1 = -2.56\pm0.50$.

Concerning L_9^r and L_{10}^r we have used the mean value of the following determinations:

$$
L_9^r(M_\rho) = \begin{cases} 5.93\pm0.43\times10^{-3}\ [49]\,, \\ \frac{F_\pi^2}{2M_\rho^2} = 7.08\pm0.40\times10^{-3}\ [24,38]\,, \\ \frac{5}{2\sqrt{6}}\frac{1}{16\pi^2} = 6.46\pm0.40\times10^{-3}\ [50,51]\,, \end{cases} \tag{B.1}
$$

$$
L_{10}^r(M_\rho) = \begin{cases} -5.13\pm0.19\times10^{-3}\ [52]\,, \\ -\frac{F_\pi^2(M_\rho^2+M_{a_1}^2)}{4M_\rho^2 M_{a_1}^2} = -5.31\pm0.40\times10^{-3}\ [38]\,, \\ -\frac{15}{8\sqrt{6}}\frac{1}{16\pi^2} = -4.85\pm0.40\times10^{-3}\ [50,51]\,. \end{cases} \tag{B.2}
$$

Appendix C: Determination of C_{80}^r

The constant C_{80}^r in (27) can be determined via resonance saturation by use of mass and decay constant differences of the axial-vector mesons a_1 and K_1. The relevant terms of the resonance Lagrangian [39] are

$$
\begin{aligned}
\mathcal{L}_\mathrm{R} = &\frac{M_{a_1}^2}{4}\langle A_{\mu\nu}A^{\mu\nu}\rangle + \lambda_6^{AA}\langle\chi_+ A_{\mu\nu}A^{\mu\nu}\rangle \\
&+\lambda^{SAA}\langle S A_{\mu\nu}A^{\mu\nu}\rangle + \frac{F_A}{2\sqrt{2}}\langle A_{\mu\nu}f_-^{\mu\nu}\rangle \\
&+\lambda_2^{SA}\langle\{S,A_{\mu\nu}\}f_-^{\mu\nu}\rangle - \frac{1}{2}M_S^2\langle S^2\rangle \\
&+c_d\langle S u^\mu u_\mu\rangle + c_m\langle S\chi_+\rangle\,,
\end{aligned} \tag{C.1}
$$

where the antisymmetric tensor field $A_{\mu\nu}$ contains the axial-vector mesons and S includes the scalar mesons. One obtains the following expression for C_{80} [39]:

$$
\begin{aligned}
C_{80}^r = F^2\Bigg(&\frac{c_d c_m}{2M_S^4} + \frac{1}{2}\Bigg(\lambda_6^{AA}\frac{F_A^2}{M_{a_1}^4} - 2\sqrt{2}\lambda_2^{SA}\frac{F_A c_m}{M_{a_1}^2 M_S^2} \\
&+\lambda^{SAA}\frac{F_A^2 c_m}{M_{a_1}^4 M_S^2}\Bigg)\Bigg)\,.
\end{aligned} \tag{C.2}
$$

In analogy to the notation in [33] we define

$$
e_A^m = 2\left(\lambda_6^{AA} + \frac{c_m}{M_S^2}\lambda^{SAA}\right), \tag{C.3}
$$

$$
f_{A1}^m = M_{a_1}\frac{c_m}{M_S^2}\lambda_2^{SA}\,. \tag{C.4}
$$

The physical $K_1(1270)$ and $K_1(1400)$ states are a mixture of the $J^{PC}=1^{++}$ and 1^{+-} states K_{1A} and K_{1B}:

$$
\begin{aligned}
K_1(1270) &= K_{1A}\sin\theta + K_{1B}\cos\theta\,,\\
K_1(1400) &= K_{1A}\cos\theta - K_{1B}\sin\theta\,.
\end{aligned} \tag{C.5}
$$

With a mixing angle θ of $(59\pm3)^\circ$ [53] the mass of the K_{1A} state is given by

$$M_{K_{1A}} = 1308 \pm 10\,\mathrm{MeV}\,. \tag{C.6}$$

There is the following relation [54, 55] between the decay constants of the K_{1A} and the $K_1(1270)$:

$$F_{K_{1A}} = \frac{F_{K_1(1270)}}{\sin\theta - \delta\cos\theta} = 159 \pm 20\,\mathrm{MeV}\,, \tag{C.7}$$

with [54]

$$\delta = \frac{1}{\sqrt{2}}\frac{m_s - m_u}{m_s + m_u} \approx 0.16\,. \tag{C.8}$$

One obtains values for e^m_A and $f^m_{A\,1}$ via the relations

$$M_{K_{1A}} - M^{ph}_{a_1} = 4e^m_A B_0(m_s - (m_u + m_d)/2) \tag{C.9}$$

and

$$F_{K_{1A}} - F_{a_1} = \frac{8\sqrt{2}f^m_{A\,1}}{M^{ph}_{a_1}} B_0(m_s - (m_u + m_d)/2)\,. \tag{C.10}$$

Together with $F_{a_1} = 165 \pm 13\,\mathrm{MeV}$ [46], $M^{ph}_{a_1} = 1230 \pm 40\,\mathrm{MeV}$ and $m_s = 25.90 m_u$, this leads to

$$C^r_{80} = (1.8 \pm 0.4) \times 10^{-5}\,. \tag{C.11}$$

References

1. Particle Data Group, W.-M. Yao et al., J. Phys. G **33**, 1 (2006)
2. M.V. Chizhov, Mod. Phys. Lett. A **8**, 2753 (1993) [arXiv: hep-ph/0401217]
3. A.V. Chernyshev, A.B. Krasulin, V.D. Laptev, V.A. Matveev, M.D. Cooper, Mod. Phys. Lett. A **12**, 1669 (1997)
4. S. Weinberg, Physica A **96**, 327 (1979)
5. J. Gasser, H. Leutwyler, Ann. Phys. **158**, 142 (1984)
6. J. Gasser, H. Leutwyler, Nucl. Phys. B **250**, 465 (1985)
7. H. Leutwyler, Ann. Phys. **235**, 165 (1994) [arXiv:hep-ph/9311274]
8. G. 't Hooft, Nucl. Phys. B **72**, 461 (1974)
9. J. Bijnens, P. Talavera, Nucl. Phys. B **489**, 387 (1997) [arXiv:hep-ph/9610269]
10. C.Q. Geng, I.L. Ho, T.H. Wu, Nucl. Phys. B **684**, 281 (2004) [arXiv:hep-ph/0306165]
11. E.A. Kuraev, Yu.M. Bystritsky, Phys. Rev. D **69**, 114 004 (2004) [arXiv:hep-ph/0310275]
12. E. Frlez, Nucl. Phys. Proc. Suppl. **162**, 148 (2006) [arXiv: hep-ex/0606023]
13. A. Bay et al., Phys. Lett. B **174**, 445 (1986)
14. SINDRUM Collaboration, S. Egli et al., Phys. Lett. B **222**, 533 (1989)
15. V.N. Bolotov et al., Phys. Lett. B **243**, 308 (1990)
16. J. Wess, B. Zumino, Phys. Lett. B **37**, 95 (1971)
17. E. Witten, Nucl. Phys. B **223**, 422 (1983)
18. S. Weinberg, Physica A **96**, 327 (1979)
19. J. Bijnens, G. Colangelo, G. Ecker, JHEP **9902**, 020 (1999) [arXiv:hep-ph/9902437]
20. T. Ebertshauser, H.W. Fearing, S. Scherer, Phys. Rev. D **65**, 054 033 (2002) [arXiv:hep-ph/0110261]
21. J. Bijnens, L. Girlanda, P. Talavera, Eur. Phys. J. C **23**, 539 (2002) [arXiv:hep-ph/0110400]
22. R. Urech, Nucl. Phys. B **433**, 234 (1995) [arXiv:hep-ph/9405341]
23. M. Knecht, H. Neufeld, H. Rupertsberger, P. Talavera, Eur. Phys. J. C **12**, 469 (2000) [arXiv:hep-ph/9909284]
24. G. Ecker, J. Gasser, A. Pich, E. de Rafael, Nucl. Phys. B **321**, 311 (1989)
25. G. Ecker, J. Gasser, H. Leutwyler, A. Pich, E. de Rafael, Phys. Lett. B **223**, 425 (1989)
26. F. Guerrero, A. Pich, Phys. Lett. B **412**, 382 (1997) [arXiv:hep-ph/9707347]
27. G.P. Lepage, S.J. Brodsky, Phys. Lett. B **87**, 359 (1979)
28. G.P. Lepage, S.J. Brodsky, Phys. Rev. D **22**, 2157 (1980)
29. S.M. Berman, Phys. Rev. Lett. **1**, 468 (1958)
30. F.E. Low, Phys. Rev. **110**, 974 (1958)
31. V. Cirigliano, G. Ecker, M. Eidemuller, R. Kaiser, A. Pich, J. Portoles, JHEP **0504**, 006 (2005) [arXiv:hep-ph/0503108]
32. S. Dürr, J. Kambor, Phys. Rev. D **61**, 114 025 (2000) [arXiv:hep-ph/9907539]
33. K. Kampf, B. Moussallam, Eur. Phys. J. C **47**, 723 (2006) [arXiv:hep-ph/0604125]
34. J. Bijnens, P. Talavera, JHEP **0203**, 046 (2002) [arXiv: hep-ph/0203049]
35. J. Prades, arXiv:0707.1789 [hep-ph]
36. KTeV Collaboration, E. Abouzaid et al., Phys. Rev. Lett. **96**, 101 801 (2006) [arXiv:hep-ex/0508010]
37. NA48 Collaboration, A. Lai et al., Eur. Phys. J. C **30**, 33 (2003)
38. V. Cirigliano, G. Ecker, M. Eidemuller, A. Pich, J. Portoles, Phys. Lett. B **596**, 96 (2004) [arXiv:hep-ph/0404004]
39. V. Cirigliano, G. Ecker, M. Eidemuller, R. Kaiser, A. Pich, J. Portoles, Nucl. Phys. B **753**, 139 (2006) [arXiv:hep-ph/0603205]
40. B. Ananthanarayan, B. Moussallam, JHEP **0205**, 052 (2002) [arXiv:hep-ph/0205232]
41. A.A. Poblaguev et al., Phys. Rev. Lett. **89**, 061 803 (2002) [arXiv:hep-ex/0204006]
42. S. Descotes-Genon, B. Moussallam, Eur. Phys. J. C **42**, 403 (2005) [arXiv:hep-ph/0505077]
43. T. Kinoshita, J. Math. Phys. **3**, 650 (1972)
44. T.D. Lee, M. Nauenberg, Phys. Rev. B **133**, 1549 (1964)
45. W.J. Marciano, A. Sirlin, Phys. Rev. Lett. **71**, 3629 (1993)
46. B. Moussallam, Nucl. Phys. B **504**, 381 (1997) [arXiv:hep-ph/9701400]
47. B. Ananthanarayan, B. Moussallam, JHEP **0406**, 047 (2004) [arXiv:hep-ph/0405206]
48. G. Amoros, J. Bijnens, P. Talavera, Nucl. Phys. B **602**, 87 (2001) [arXiv:hep-ph/0101127]
49. J. Bijnens, P. Talavera, JHEP **0203**, 046 (2002) [arXiv: hep-ph/0203049]
50. S. Peris, M. Perrottet, E. de Rafael, JHEP **9805**, 011 (1998) [arXiv:hep-ph/9805442]
51. M.F.L. Golterman, S. Peris, Phys. Rev. D **61**, 034 018 (2000) [arXiv:hep-ph/9908252]
52. M. Davier, L. Girlanda, A. Hocker, J. Stern, Phys. Rev. D **58**, 096 014 (1998) [arXiv:hep-ph/9802447]
53. D.M. Li, Z. Li, Eur. Phys. J. A **28**, 369 (2006) [arXiv: hep-ph/0606297]
54. M. Suzuki, Phys. Rev. D **47**, 1252 (1993)
55. H.Y. Cheng, Phys. Rev. D **67**, 094 007 (2003) [arXiv: hep-ph/0301198]